JOURNAL OF
EMERGING INVESTIGATORS

Article

Sustained ethanol exposure alters baseline locomotor behavior and polyQ aggregation in *C. elegans*

Philip Jeong[1], Woo Yong Jeong[1]
[1] Phillips Academy, Andover, Massachusetts

SUMMARY

Protein aggregation occurs when misfolded proteins accumulate into larger structures that can interfere with cellular function and are associated with neurodegenerative diseases such as Huntington's disease. The extent and distribution of aggregation can vary among organisms, suggesting that physiological context may shape proteostatic outcomes. We hypothesized that sustained ethanol exposure would alter aggregate-size distributions and baseline locomotor performance in *Caenorhabditis elegans*. We exposed young adult wild-type N2 animals and neuronal Q74 animals expressing yellow fluorescent protein (YFP)-tagged polyglutamine (polyQ) containing 74 glutamine repeats to 200 mM ethanol for 24 h, then assessed thrashing and neuronal aggregation after ethanol removal. Median thrashing increased in Q74 animals and decreased in N2 animals following ethanol preconditioning, but neither comparison was statistically significant (Q74: $p = 0.171$; N2: $p = 0.086$). In Q74 animals, ethanol-pretreated worms also showed lower median percent aggregate area, a visually left-shifted aggregate-size distribution, and a lower median proportion of large aggregates (operationally defined as ≥30 px²), but these comparisons were not statistically significant ($p = 0.193$, 0.182, and 0.394, respectively). These patterns suggest that sustained ethanol exposure may be associated with post-exposure differences in baseline locomotor and aggregation phenotypes in *C. elegans*.

INTRODUCTION

Proteostasis, the coordinated control of protein synthesis, folding, trafficking, and clearance, supports cellular function by limiting the accumulation of misfolded and aggregation-prone proteins over time (1, 2). When folding and clearance pathways become compromised during aging or under sustained stress, some proteins transition from soluble to detergent-insoluble states and accumulate into larger structures (3). This process is associated with neurodegenerative diseases such as Huntington's disease, in which abnormal protein aggregation can disrupt normal cellular function (1, 3, 4).

Although *Caenorhabditis elegans* does not naturally develop human neurodegenerative diseases, researchers frequently use it to model disease-related protein aggregation because it has conserved stress-response pathways, a transparent body, and a short, well-characterized lifespan (1). These features allow researchers to express human disease-associated proteins in a living organism and to observe changes in both protein aggregation and behavior. In *C. elegans*, proteostatic stressors affect the solubility of specific proteins rather than the entire proteome. Most proteins remain soluble, while aggregation-prone proteins are more susceptible to misfolding (3). Researchers can therefore treat proteostasis as a quantitative property because physiological context can alter both the extent and distribution of aggregation among individual worms (3).

Expanded polyglutamine (polyQ) tracts are abnormally long runs of glutamine residues that make proteins more prone to misfolding and aggregation (5). In humans, expanded polyQ tracts occur in proteins associated with several neurodegenerative disorders, including the huntingtin protein involved in Huntington's disease (6, 7). The Q74 strain used in this study expresses a yellow fluorescent protein (YFP)-tagged polyQ protein containing 74 glutamine repeats in neurons (5). This expanded polyQ tract produces visible fluorescent inclusions as the animals age, making Q74 a useful model for assessing how environmental conditioning shifts aggregation patterns (5, 6, 7). Because neurons are distributed throughout the body of *C. elegans*, whole-body imaging provides a way to assess neuronal aggregation across the worm rather than restricting analysis to a single region.

Because organismal physiological state influences cellular proteostasis, *in vivo* models that allow researchers to measure aggregation alongside behavior are essential for correlating aggregation patterns with functional outcomes (8). *C. elegans*, in particular, enables *in vivo* fluorescence imaging and quantitative locomotor assays within a genetically defined, developmentally stereotyped organism that retains conserved stress-response pathways (1, 7). Researchers commonly use locomotor thrashing in *C. elegans* as an integrated readout of neuromuscular and physiological state, reflecting coordinated neuronal, muscular, and metabolic activity (1, 9). Likewise, aggregation of expanded polyQ tracts in Q74 animals provides a validated *in vivo* readout of their neuronal aggregation phenotypes, capturing disease-relevant aggregation dynamics within an intact organismal context (5, 7). Pairing aggregation measurements with behavioral assays allows researchers to consider changes in protein aggregation alongside organismal function rather than in isolation (9).

One way to experimentally shift an organism's physiological state without inducing acute stress is through sustained environmental exposure. A substantial body of prior work frames ethanol and other mild stressors within hormetic or preconditioning paradigms, in which low-dose exposure induces adaptive responses that confer resilience to subsequent stimuli (10, 11). Hormesis is a biphasic dose-response relationship in which moderate stress stimulates

https://doi.org/10.59720/26-078

adaptive remodeling, whereas higher doses exceed compensatory capacity and produce toxicity (10). Prior research demonstrated that prolonged ethanol exposure can produce behavioral plasticity in *C. elegans*, including the development of ethanol preference, and that induction of this preference requires substantial internal ethanol accumulation (12). Additionally, prior studies have shown that prolonged ethanol exposure induces persistent changes in gene expression across stress-response and metabolic pathways, providing a plausible explanation for effects that persist after ethanol removal (10, 11, 13).

In Q74 *C. elegans*, aggregation develops through a sequence of intermediate protein states before larger aggregates form (5). Prior studies show that physiological conditions can shift the distribution of aggregate sizes without necessarily altering average inclusion measures (5). As a result, metrics that rely solely on averages can fail to capture critical redistribution across size classes and increased variability between individual animals (5).

It remains unclear whether prolonged ethanol exposure in the absence of acute treatment reorganizes polyQ aggregation across animals, rather than simply changing average inclusion number or size (3, 5, 12, 13). Addressing this question requires approaches that quantify aggregate-size composition and variability among individual worms. To test this, we hypothesized that sustained ethanol exposure would not only alter median aggregate measures but would also induce a redistribution of aggregate sizes and alter variability among individual worms. Pairing these analyses of polyQ aggregation with behavioral measurements further helps contextualize these distributional changes at the organismal level (9).

To evaluate these potential shifts, we subjected both N2 and Q74 *C. elegans* to a 24-h ethanol preconditioning window. We then characterized the resulting baseline locomotor behavior in both strains and assessed YFP-labeled polyQ aggregation in the Q74 strain. Using quantitative locomotor assays and fluorescence imaging, we tested whether ethanol exposure was associated with changes in aggregate-size distribution and locomotor output after ethanol removal. Crucially, we performed all assays following transfer to ethanol-free conditions and in the absence of acute oxidative challenge, thereby allowing for isolation of baseline states after exposure (1, 3, 5, 9). Median thrashing shifted upward in ethanol-pretreated Q74 animals and downward in ethanol-pretreated N2 animals, although neither within-genotype comparison reached statistical significance. In Q74 animals, ethanol-pretreated worms also showed lower median percent aggregate area and fewer large aggregates, but the corresponding comparisons were not statistically significant. These findings suggest that an organism's environmental history may influence baseline aggregation and locomotor phenotypes measured after the stimulus is removed.

RESULTS

Baseline locomotor patterns following ethanol preconditioning in N2 and Q74 *C. elegans*

To assess baseline locomotor behavior following sustained ethanol preconditioning in N2 and Q74 strains of *C. elegans*, we quantified thrashing activity using a standard assay in which we counted body bends over a 30 s interval (9). The Q74 strain is a neuronal polyQ model that expresses a YFP-tagged polyQ protein containing 74 glutamine repeats.

Q74 control animals displayed a median thrashing rate of 25.0 thrashes per 30 s (IQR = 22.5–25.5; n = 4), while ethanol-pretreated Q74 animals exhibited a median of 28.5 thrashes per 30 s (IQR = 26.0–35.5; n = 4); this difference was not statistically significant (Mann-Whitney U = 3.0, p = 0.171; **Figure 1**). In contrast, N2 control animals showed a median thrashing rate of 55.5 thrashes per 30 s (IQR = 54.0–63.0; n = 4), whereas ethanol-pretreated N2 animals had a median of 33.5 thrashes per 30 s (IQR = 25.5–46.5; n = 4); however, the difference between control and ethanol-treated N2 animals was not statistically significant (U = 1.5, p = 0.086; **Figure 1**). Thus, median thrashing shifted in opposite directions in Q74 and N2 animals following ethanol preconditioning, although neither within-genotype comparison reached statistical significance.

Neuronal polyQ percent aggregate area following ethanol preconditioning in Q74 *C. elegans*

We next assessed neuronal polyQ aggregation in Q74 animals by measuring the percentage of each individual worm's area occupied by discrete fluorescent puncta. We assessed aggregation only in Q74 *C. elegans* because the assay relied on the fluorescently tagged Q74 protein expressed by this strain. Because N2 *C. elegans* do not express this protein, we excluded them from the aggregation analysis.

Q74 *C. elegans* control animals had a median percent aggregate area of 8.3% (IQR = 6.0–12.8%; n = 6), whereas ethanol-pretreated Q74 animals had a median of 6.3% (IQR = 5.6–6.8%; n = 6); this difference was not statistically significant (Mann-Whitney U = 9.5, p = 0.193; **Figures 2, 3**). The ethanol-pretreated group therefore showed a lower observed median and narrower IQR, but the comparison did not provide evidence of a statistically significant treatment effect.

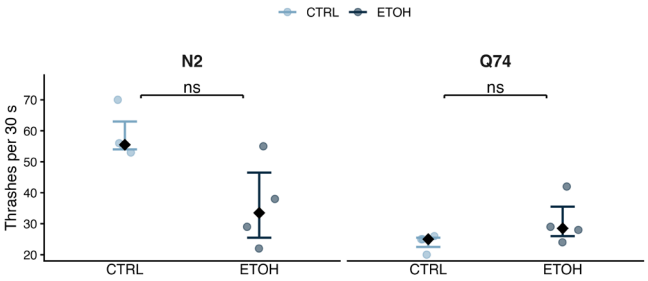

Figure 1: Locomotor output following ethanol preconditioning in N2 and Q74 *Caenorhabditis elegans* strains. Baseline locomotor activity was quantified using a thrashing assay following 24-h ethanol preconditioning. Q74 and N2 animals were exposed to ethanol-supplemented plates (200 mM) or control plates prior to thrashing assessment, and thrashing rates were measured under ethanol-free baseline conditions. Individual points represent single animals. Black diamond markers denote group medians, with vertical error bars indicating the interquartile range (IQR) (n = 4 animals per condition). Control and ethanol-pretreated groups within each genotype were compared using two-sided exact permutation Mann-Whitney U tests (Q74: U = 3.0, p = 0.171; N2: U = 1.5, p = 0.086).

https://doi.org/10.59720/26-078

Aggregate-size distributions following ethanol preconditioning in Q74 *C. elegans*

To assess polyQ aggregation beyond overall percent aggregate area following ethanol preconditioning, we analyzed the sizes of individual fluorescent puncta in Q74 *C. elegans*.

Aggregate-area histograms showed a visually left-shifted pattern in ethanol-pretreated Q74 *C. elegans* relative to untreated controls (**Figure 4**). Ethanol-pretreated Q74 *C. elegans* had a higher frequency of small-area puncta and a lower frequency of larger aggregates, while control Q74 *C. elegans* displayed a broader distribution with a more pronounced rightward tail (**Figure 4**). These distributions included 614 puncta from control animals and 511 puncta from ethanol-pretreated animals (n = 6 per group). The pooled aggregate-area distributions were not statistically distinguishable using the Kolmogorov-Smirnov statistic (D = 0.149, worm-level permutation p = 0.182).

We also examined the pattern at the level of individual animals. Control animals had a median of 17.3% large aggregates (≥30 px^2; IQR = 4.3–27.2%; n = 6), whereas ethanol-pretreated animals had a median of 8.2% (IQR = 7.2–9.0%; n = 6); this difference was not statistically significant (Mann-Whitney U = 12.0, p = 0.394; **Figure 5**). The narrower IQR in ethanol-pretreated animals indicates less dispersion in the observed values. We did not include N2 *C. elegans* in this analysis because they do not express the fluorescent Q74 polyQ protein required to identify and measure individual polyQ puncta. Together, these results show a visual pattern of fewer large aggregates and less dispersion among ethanol-pretreated Q74 animals, although the between-group comparison did not reach statistical significance (**Figures 4, 5**).

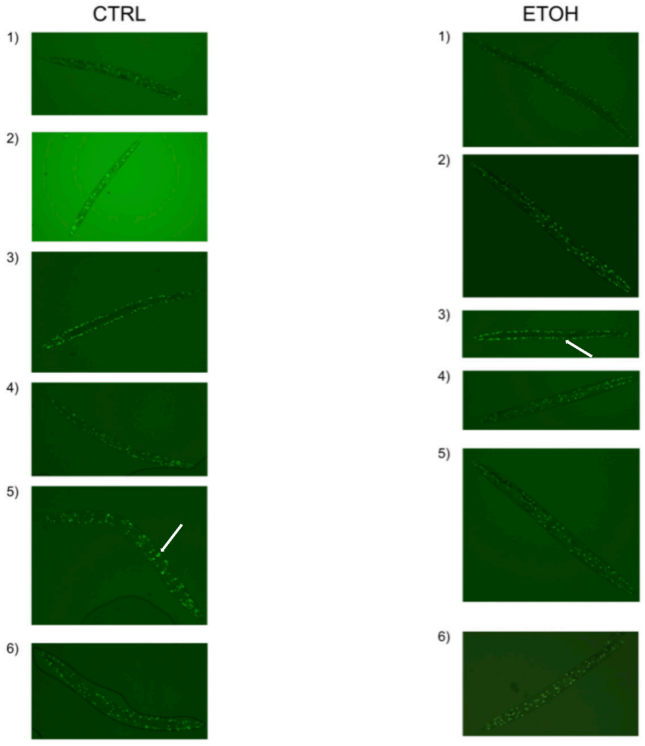

Figure 2: Representative fluorescence micrographs of neuronal polyglutamine (polyQ) aggregation in Q74 *Caenorhabditis elegans* following ethanol preconditioning. Fluorescence micrographs show yellow fluorescent protein (YFP)-tagged polyglutamine aggregation in individual Q74 animals following 24-h exposure to control (CTRL) or ethanol-supplemented (ETOH; 200 mM) plates. YFP-tagged polyQ puncta were imaged at 40× optical magnification on a fluorescence microscope using identical processing settings across conditions. Images correspond to the individual animals quantified and illustrate representative aggregate patterns underlying per-animal summary metrics. White arrows indicate representative larger and smaller fluorescent puncta in the control and ethanol-pretreated conditions, respectively.

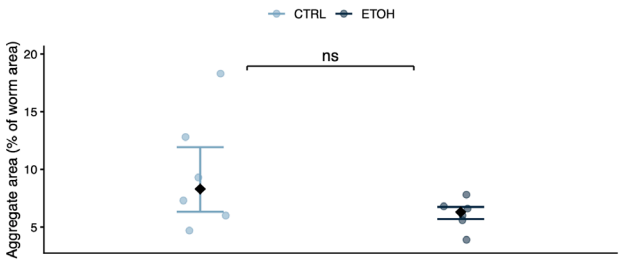

Figure 3: Neuronal polyglutamine (polyQ) percent aggregate area following ethanol preconditioning in Q74 *Caenorhabditis elegans*. Day-1 adult Q74 animals were exposed to control plates or plates containing 200 mM ethanol for 24 h and subsequently imaged under ethanol-free conditions. Percent aggregate area was quantified from fluorescence micrographs as the percentage of each worm's imaged area occupied by fluorescent polyQ puncta. Individual points represent single animals (n = 6 per condition); black diamonds indicate group medians, and vertical error bars indicate interquartile ranges (IQRs). Control and ethanol-pretreated groups were compared using a two-sided exact permutation Mann-Whitney U test (U = 9.5, p = 0.193).

DISCUSSION

In this study, we examined whether sustained ethanol preconditioning was associated with changes in baseline locomotor behavior and aggregation phenotypes in a neuronal polyQ model of *C. elegans*. We hypothesized that ethanol preconditioning would induce changes in the proteostasis network that would remain detectable after the removal of ethanol.

Following ethanol preconditioning, Q74 animals showed a higher median thrashing rate than Q74 controls, whereas N2 animals showed a lower median thrashing rate than N2 controls; neither within-genotype comparison reached statistical significance. The opposite directional patterns observed in the two strains may reflect differences in their underlying physiological states. Q74 *C. elegans* express an aggregation-prone polyQ protein containing 74 glutamine repeats in neurons, which may alter neuronal proteostasis and the way the neuromuscular system responds to sustained ethanol exposure, whereas N2 *C. elegans* do not express this protein. However, because we did not directly test a treatment-by-genotype interaction or measure neuronal signaling or stress-response pathways, we cannot conclude that ethanol's effect differed significantly by genotype or determine the mechanism underlying the observed pattern.

https://doi.org/10.59720/26-078

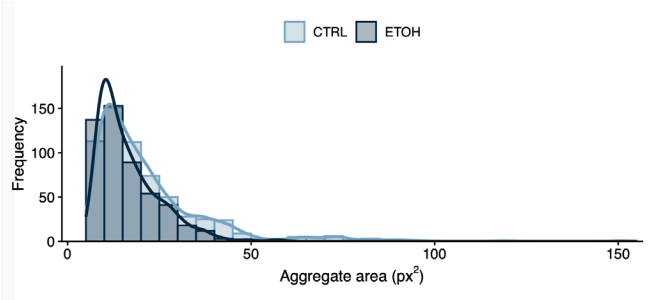

Figure 4: Polyglutamine aggregate-size distributions in control and ethanol-pretreated Q74 *Caenorhabditis elegans*. Day-1 adult Q74 animals were exposed to control plates or plates containing 200 mM ethanol for 24 h before fluorescence imaging under ethanol-free conditions. Histogram overlays show the distribution of individual polyglutamine aggregate areas measured from fluorescence micrographs of Q74 C. elegans under control (CTRL) and ethanol-pretreated (ETOH) conditions. Aggregate area was quantified as the pixel area (px²) of individual fluorescent puncta. Histograms represent pooled puncta for visualization only (CTRL: 614 puncta from 6 animals; ETOH: 511 puncta from 6 animals). Individual worms, rather than individual puncta, were treated as the biological replicates. Kernel density estimates are overlaid to visualize the distribution's shape. The separation between pooled aggregate-area distributions was quantified using the two-sample Kolmogorov-Smirnov statistic, with statistical significance evaluated by a worm-level permutation procedure that preserved all puncta within their original worm ($D = 0.149$, worm-level permutation $p = 0.182$).

Prior work in *C. elegans* has shown that ethanol acts as a conditioning stimulus that alters locomotor plasticity, reflecting changes in the neural control of movement following prior environmental exposure. However, many existing studies assess these responses during acute oxidative challenges or immediately following stress (12). In our study, we measured baseline locomotion after transferring the animals to ethanol-free conditions. Although neither within-genotype comparison reached statistical significance, the directional patterns observed after transfer to ethanol-free conditions raise the possibility that prior ethanol exposure may have lingering effects on baseline locomotor state. Examining these lingering effects provides a complementary perspective to studies that focus only on immediate stress responses (10, 11).

Our second main finding indicates that ethanol preconditioning is associated with a lower median neuronal polyQ percent aggregate area in Q74 *C. elegans* and a redistribution of aggregate sizes. Specifically, ethanol-pretreated animals showed a pattern toward smaller aggregates and attenuation of the high-aggregate tail of the distribution. Although these comparisons did not reach statistical significance ($p = 0.193$, 0.182, and 0.394, respectively), the observed patterns are consistent with previous studies showing that physiological context influences how aggregate states are distributed across individual worms and suggest that similar patterns may be detectable following environmental preconditioning (3).

Rather than presenting our results as binary outcomes (protein aggregation vs. no aggregation), we interpret them through a distributional lens to assess whether ethanol shifts the distribution of aggregate size. We observed a pattern in which ethanol-pretreated Q74 *C. elegans* had fewer large aggregates, which are often associated with functional impairment, although the large-aggregate comparison was not statistically significant (4, 6). Because we measured locomotor and aggregation phenotypes in independent cohorts, we cannot infer a direct relationship between these outcomes. The observed distributional pattern may nevertheless be consistent with a modified proteostatic state in which the relative abundance of different aggregation states, rather than aggregate presence alone, is relevant to functional outcomes (3, 4). While this study does not identify the specific pathways responsible for clearing proteins, the data suggest that ethanol exposure may be associated with a reorganization of aggregate size and distribution, rather than simply eliminating them.

This observed distributional pattern aligns with the principle that physiological states can shift dramatically without producing irreversible damage. For example, sublethal stress can induce reversible suppression of locomotion through coordinated redox regulation rather than destabilizing the entire proteome (2). Accordingly, we interpret our data as suggestive of a possible shift in baseline aggregation phenotypes following ethanol preconditioning and a possible change in how cells manage aggregation-prone proteins (9). Future studies may examine whether the distribution shifts back to its original state with time or other reversible conditions.

Several factors limit our ability to identify the specific biological mechanisms responsible for these findings. First, we conducted imaging-based aggregation analyses and locomotor assays on a limited number of animals (locomotor $n = 16$; imaging $n = 12$). Given the small sample size and our limited ability to assess the underlying distributions reliably, we used two-sided exact permutation Mann-Whitney U tests to compare ethanol-pretreated and control groups within each genotype. The small sample size limited statistical power to detect small shifts in aggregate populations or statistically significant behavioral trends. Although we applied the same

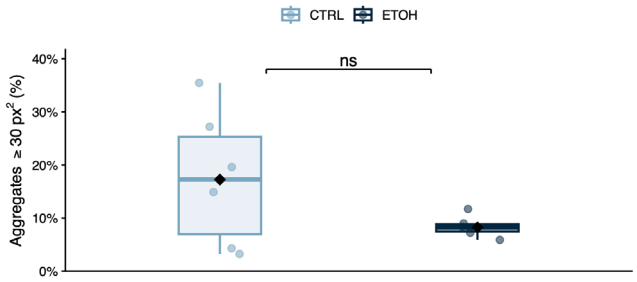

Figure 5: Percentage of large polyglutamine aggregates in control and ethanol-pretreated Q74 *Caenorhabditis elegans*. Day-1 adult Q74 animals were exposed to control plates or plates containing 200 mM ethanol for 24 h before fluorescence imaging under ethanol-free conditions. Box plots with jittered points show the percent of polyglutamine aggregates with areas ≥30 px² for individual control (CTRL) and ethanol-pretreated (ETOH) Q74 C. elegans ($n = 6$ per condition). Boxes represent the interquartile range (IQR), center lines and black diamond markers indicate group medians, and each point represents a single animal. Control and ethanol-pretreated groups were compared using a two-sided exact permutation Mann-Whitney U test ($U = 12.0$, $p = 0.394$).

https://doi.org/10.59720/26-078

scoring criteria and assay conditions across all groups, blinded or video-based locomotor quantification would improve accuracy in future studies. Moreover, we assessed locomotor and aggregation phenotypes in independent cohorts, preventing direct within-animal comparison of locomotor and aggregation outcomes. Because we measured multiple puncta within each worm, we evaluated statistical significance for the Kolmogorov-Smirnov statistic using a worm-level permutation procedure that kept all points from each worm grouped together. Future studies should also examine multiple ethanol concentrations and include a time course after ethanol removal. Additionally, because we could not confirm the position of the YFP tag relative to the Q74 tract, we cannot exclude the possibility that the fluorescent tag influenced the aggregation behavior measured in this study. Finally, the absence of transcriptional reporters or genetic perturbations limits our ability to determine whether specific stress-response transcription factors contributed to the observed phenotypes (9, 14).

Collectively, these findings suggest that ethanol preconditioning may be associated with differences in baseline locomotor and aggregation phenotypes in *C.* elegans. By pairing behavioral assays with distribution-based aggregation analyses, this proof-of-principle study provides a framework for testing how sustained environmental inputs influence proteostatic phenotypes *in vivo*. Future studies can identify the specific mechanisms through which prolonged conditioning stimuli modify aggregation dynamics and neuromuscular health. PolyQ expansions are a hallmark of neurodegenerative conditions such as Huntington's disease (7). Understanding how prolonged versus acute stress shapes aggregation may offer new insights into environmental modifiers of disease progression (7).

MATERIALS AND METHODS

Model organism, strains, and general maintenance

Experiments were conducted using wild-type Bristol N2 worms and the neuronal Q74 polyQ aggregation model, which expresses a YFP-tagged polyQ protein containing 74 glutamine repeats in neurons and models polyQ aggregation associated with neurodegenerative diseases (5).

C. elegans populations were maintained at 20 °C on 35- and 90-mm Nematode Growth Medium (NGM)-lite agar plates seeded with mCherry-tagged *Escherichia coli* OP50 under standard laboratory conditions (1, 15). All experiments were performed using synchronized day-1 adult animals to minimize age-dependent variability in locomotor performance and aggregation phenotypes, which are known to change rapidly across adulthood (15, 16). Unless otherwise noted, all handling and assays were carried out at room temperature in accordance with established *C. elegans* thrashing and imaging assay protocols (16).

Synchronization and staging

C. elegans populations were synchronized to ensure controlled aging and avoid confounding effects of developmental heterogeneity (1, 15, 16). A mixed-age worm population was obtained, bleached with a freshly prepared alkaline sodium hypochlorite solution, and then extensively rinsed in sterile M9 buffer, a standard saline solution used for handling and washing *C. elegans,* to isolate the embryos. Embryos were then allowed to hatch and develop on standard NGM-lite plates seeded with *E. coli* OP50 until reaching young adulthood. To suppress progeny production during locomotor thrashing and imaging assays, animals were transferred to plates containing 80 µM 5-fluoro-2'-deoxyuridine (FUDR) after reaching adulthood (15, 16).

Animals displaying injury, abnormal morphology, or cuticle damage were excluded from analysis. Additionally, plates were inspected prior to assays for signs of contamination or desiccation, and any compromised plates were excluded before cohorting.

Ethanol preconditioning paradigm

Day-1 adult *C. elegans* were exposed for 24 h to NGM-lite treatment plates containing a nominal ethanol concentration of 200 mM prior to all locomotor thrashing and aggregation assays. This sustained 24-h ethanol preconditioning window was selected to promote internal ethanol accumulation and ethanol-specific physiological adaptation rather than transient suppression of locomotor activity in *C. elegans* (12). The nominal concentration of 200 mM was selected as a conservative dose within the 200–400 mM range used in prior sustained ethanol-exposure studies in *C.* elegans. Prolonged exposure to 300 mM ethanol has been shown to produce internal ethanol accumulation and behavioral plasticity without completely suppressing locomotion, while 200 mM has been used in chronic developmental ethanol-exposure studies examining longer-term molecular responses (12, 17). Treatment plates were freshly surface-spiked with ethanol to a final concentration of 200 mM immediately before adding animals. After 24 h of plate-based ethanol exposure, worms were thoroughly washed in sterile M9 buffer to remove residual surface ethanol and then transferred to ethanol-free M9 buffer prior to all subsequent assays. Control plates were handled identically, but in the absence of ethanol.

To minimize environmental variability, control and ethanol-treated plates were placed side by side and were processed in parallel throughout the 24-h exposure window. Two independent sets of cohorts were prepared for locomotor measurements and imaging-based aggregation analyses.

Locomotor thrashing assay

Locomotor performance was quantified using a thrashing assay, which provides a sensitive readout of baseline neuromuscular function in adult *C. elegans* (9). This assay was performed on both Q74 and N2 animals.

Following washing, the worms were transferred into 10 µL droplets of ethanol-free M9 for thrashing assessment. Body bends (thrashes) were defined as a complete change in body bend direction (mid-body curvature from one side to the other) and were counted manually by eye over a single 30 s interval. For each genotype-treatment condition (Q74 control, Q74 ethanol-pretreated, N2 control, and N2 ethanol-pretreated), thrashing was measured in n = 4 individual worms (total n = 16).

Because the small group sizes did not allow distributional assumptions to be established reliably, data were summarized using medians and interquartile ranges (IQRs). Ethanol-treated and control groups were compared within each

https://doi.org/10.59720/26-078

genotype using two-sided exact permutation Mann-Whitney U tests, with average ranks assigned to tied values and statistical significance assessed at $p < 0.05$.

Thrashing measurements were not blinded to treatment; however, scoring criteria and assay conditions were held constant across groups, including room temperature, droplet volumes, and timing.

Fluorescence imaging of neuronal polyQ aggregation

Neuronal polyQ percent aggregate area in control and ethanol-pretreated Q74 animals was quantified using fluorescence micrographs. Fluorescence imaging captures heterogeneity in aggregate burden and size that binary presence/absence labels do not resolve (5).

Following ethanol or control plate exposure, Q74 worms (control $n = 6$, treated $n = 6$) were immobilized using levamisole (100 mM) and imaged at 40× optical magnification. Fluorescence micrographs were acquired for subsequent quantification of neuronal polyQ aggregation.

To examine variation in polyQ aggregate morphology, regions of interest were defined as encompassing the entire worm body. At the start of each imaging session, the exposure time and gain were adjusted to obtain a clear, unsaturated YFP signal, and then the acquisition settings were held constant for all control and ethanol-treated animals imaged in that session. Images containing saturated pixels in the YFP channel were excluded or re-captured to prevent distortion of area-based measurements.

Image segmentation and aggregate size analysis

Image analysis of aggregates was performed in Fiji/ImageJ using a fixed, pre-specified segmentation pipeline applied uniformly to all images that measured the percent of each individual worm's area occupied by discrete fluorescent puncta. When multiple animals appeared within a single field of view, we manually isolated worms prior to analysis to ensure each animal was quantified independently. Each frame was converted to 8-bit format, had the background subtracted using a rolling-ball radius of 20 px, was blurred using Gaussian filtering (1 px), thresholded using Otsu's method, and had watershed segmentation applied to separate adjacent puncta. Small noise objects were excluded using a minimum size threshold, and the influence of occasional merged regions on summary measurements was reduced using a maximum size threshold.

Particle analysis was conducted using a size filter of 8–300 px^2, circularity 0.15–1.00, and edge exclusions. Manual painting or hand-correction within regions of interest was not permitted; frames requiring manual editing were excluded prior to analysis. The percent aggregate area was then quantified as the percentage of the total worm area occupied by aggregates.

For a secondary descriptive analysis, we operationally classified puncta with areas ≥30 px^2 as large aggregates because this threshold separated the sparsely populated upper tail of the observed aggregate-size distribution from the main body of puncta sizes. We did not interpret this threshold as a biologically established boundary.

Dataset assembly and statistical analysis

To visualize the distribution of aggregate sizes across treatment groups, pooled histogram overlays with kernel density estimates were generated. The separation between pooled aggregate-area distributions was quantified using the two-sample Kolmogorov-Smirnov statistic. Because multiple puncta were measured from each worm, statistical significance was evaluated using an exact worm-level permutation test in which treatment labels were permuted across the 12 worms while puncta remained grouped within their original worm. All 924 possible balanced assignments of six worms per group were evaluated.

For neuronal percent aggregate area and the percentage of large aggregates (≥30 px^2), per-worm measurements were summarized using medians and interquartile ranges (IQRs) and compared between control and ethanol-pretreated Q74 animals ($n = 6$ per condition) using two-sided exact permutation Mann-Whitney U tests, with average ranks assigned to tied values. Statistical significance was assessed at $p < 0.05$.

All statistical analyses and quantitative figure generation were performed in R (version 4.5.2). Data manipulation was performed using dplyr (version 1.2.1), and figures were generated using ggplot2 (version 4.0.3) and scales (version 1.4.0). The Mann-Whitney U tests and Kolmogorov-Smirnov statistic were implemented using custom R code. The experimental workflow schematic shown in **Figure 6** was created manually in Canva using non-generative elements.

ACKNOWLEDGMENTS

The authors thank the Brown University Pre-College laboratory program instructional staff for providing laboratory training, facilities, and the *C. elegans* strains used in this study. While data collection was initiated during the program, the experimental hypotheses, data analysis, distribution modeling, and manuscript preparation were developed independently by the authors following the program's conclusion. No external funding was received for this work.

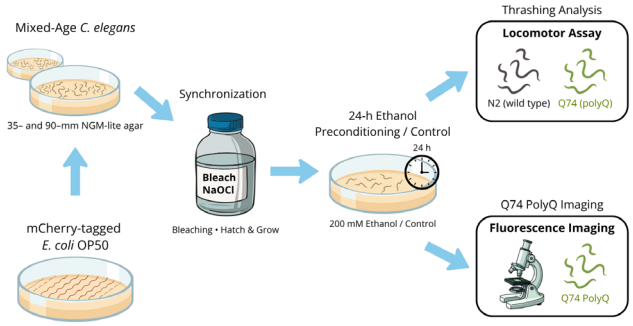

Figure 6: Experimental workflow for *Caenorhabditis elegans* synchronization and ethanol preconditioning for locomotor and fluorescence imaging assays. Mixed-age *C. elegans* populations were synchronized by alkaline hypochlorite (NaOCl) bleaching and maintained on Nematode Growth Medium (NGM)-lite agar plates seeded with mCherry-tagged *Escherichia coli* OP50. Synchronized day-1 adult animals were subjected to a 24-h, 200 mM ethanol preconditioning window before being allocated to respective assay cohorts. Locomotor thrashing assays were performed on both N2 and Q74 *C. elegans*, while fluorescence imaging of yellow fluorescent protein (YFP)-labeled polyglutamine (polyQ) aggregates was conducted only with Q74 C. elegans.

https://doi.org/10.59720/26-078

Received: April 4, 2026
Accepted: October 4, 2026
Published: November 27, 2026

REFERENCES

1. Corsi, Ann K. "A Transparent Window into Biology: A Primer on *Caenorhabditis elegans*." *WormBook*, June 2015, pp. 1–31. https://doi.org/10.1895/wormbook.1.177.1.
2. Kumsta, Caroline, *et al*. "Effects of Oxidative Stress on Behavior, Physiology, and the Redox Thiol Proteome of *Caenorhabditis elegans*." *Antioxidants & Redox Signaling*, vol. 14, no. 6, 15 Mar. 2011, pp. 1023–37. https://doi.org/10.1089/ars.2010.3203.
3. David, Della C., *et al*. "Widespread Protein Aggregation as an Inherent Part of Aging in *C. elegans*." *PLOS Biology*, vol. 8, no. 8, 10 Aug. 2010, pp. 1–23. https://doi.org/10.1371/journal.pbio.1000450.
4. Boasquívis, Patrícia Ferreira, *et al*. "Guarana (*Paullinia cupana*) Extract Protects *Caenorhabditis elegans* Models for Alzheimer disease and Huntington disease through Activation of Antioxidant and Protein Degradation Pathways." *Oxidative Medicine and Cellular Longevity*, vol. 2018, no. 1, 04 July 2018, pp. 1–16. https://doi.org/10.1155/2018/9241308.
5. Kokona, Bashkim, *et al*. "Studying Polyglutamine Aggregation in *Caenorhabditis elegans* Using an Analytical Ultracentrifuge Equipped with Fluorescence Detection." *Protein Science*, vol. 25, no. 3, 08 Dec. 2016, pp. 605–17. https://doi.org/10.1002/pro.2854.
6. Morley, James F., *et al*. "The Threshold for Polyglutamine-Expansion Protein Aggregation and Cellular Toxicity Is Dynamic and Influenced by Aging in *Caenorhabditis elegans*." *Proceedings of the National Academy of Sciences of the United States of America*, vol. 99, no. 16, 16 July 2002, pp. 10417–22. https://doi.org/10.1073/pnas.152161099.
7. Torres, Angie K., *et al*. "Studying the Mechanisms of Neurodegeneration: *C. elegans* Advantages and Opportunities." *Frontiers in Cellular Neuroscience*, vol. 19, 25 Mar. 2025, pp. 1–20. https://doi.org/10.3389/fncel.2025.1559151.
8. Morimoto, Richard I. "Cell-Nonautonomous Regulation of Proteostasis in Aging and Disease." *Cold Spring Harbor Perspectives in Biology*, vol. 12, no. 4, 08 Apr. 2019, pp. 1–20. https://doi.org/10.1101/cshperspect.a034074.
9. Bar-Ziv, Raz, *et al*. "Measurements of Physiological Stress Responses in *C. elegans*." *Journal of Visualized Experiments (JoVE)*, no. 159, 21 May 2020. https://doi.org/10.3791/61001.
10. Mattson, Mark P. "Hormesis Defined." *Ageing Research Reviews*, vol. 7, no. 1, 15 Jan. 2008, pp. 1–7. https://doi.org/10.1016/j.arr.2007.08.007.
11. Wan, Yantong, *et al*. "Current Advances and Future Trends of Hormesis in Disease." *npj Aging*, vol. 10, no. 1, 15 May 2024, pp. 1–19. https://doi.org/10.1038/s41514-024-00155-3.
12. Lee, J., *et al*. "Ethanol Preference in *C. elegans*." *Genes, Brain and Behavior*, vol. 8, no. 6, 03 Aug. 2009, pp. 578–85. https://doi.org/10.1111/j.1601-183X.2009.00513.x.
13. Sterken, Mark G., *et al*. "Transcriptional Analysis of the Response of *C. elegans* to Ethanol Exposure." *Scientific Reports*, vol. 11, no. 1, 26 May 2021, pp. 1–12. https://doi.org/10.1038/s41598-021-90282-8.
14. Zhu, An, *et al*. "Oxidation and Antioxidation of Natural Products in the Model Organism *Caenorhabditis elegans*." *Antioxidants*, vol. 11, no. 4, 01 Apr. 2022, pp. 1–29. https://doi.org/10.3390/antiox11040705.
15. Senchuk, Megan M., *et al*. "Measuring Oxidative Stress in *Caenorhabditis elegans*: Paraquat and Juglone Sensitivity Assays." *Bio-Protocol*, vol. 7, no. 1, 05 Jan. 2017, pp. 1–11. https://doi.org/10.21769/BioProtoc.2086.
16. Wu, Ziyun, *et al*. "Mitochondrial Unfolded Protein Response Transcription Factor ATFS-1 Promotes Longevity in a Long-Lived Mitochondrial Mutant through Activation of Stress Response Pathways." *BMC Biology*, vol. 16, no. 1, 18 Dec. 2018, pp. 1–19. https://doi.org/10.1186/s12915-018-0615-3.
17. Peltonen, Juhani, *et al*. "Chronic Ethanol Exposure Increases Cytochrome P-450 and Decreases Activated in Blocked Unfolded Protein Response Gene Family Transcripts in *Caenorhabditis elegans*." *Journal of Biochemical and Molecular Toxicology*, vol. 27, no. 4, 04 Feb. 2013, pp. 219–28. https://doi.org/10.1002/jbt.21473.

Copyright: © 2026 Jeong and Jeong. All JEI articles are distributed under the Creative Commons Attribution Noncommercial No Derivatives 4.0 International License. This means that you are free to share, copy, redistribute, remix, transform, or build upon the material for any purpose, provided that you credit the original author and source, include a link to the license, indicate any changes that were made, and make no representation that JEI or the original author(s) endorse you or your use of the work. The full details of the license are available at https://creativecommons.org/licenses/by-nc-nd/4.0/deed.en.